THE JOURNAL OF PHYSICAL CHEMISTRY A

Article

pubs.acs.org/JPCA

Solid-State ^{13}C NMR Investigations of Cyclophanes: [2.2] Paracyclophane and 1,8-Dioxa[8](2,7)pyrenophane

Merrill D. Halling,[a] Kiran Sagar Unikela,[b] Graham J. Bodwell,[b] David M. Grant,*[,a] and Ronald J. Pugmire*[,a]

[a]Department of Chemistry, University of Utah, Salt Lake City, Utah 84112, United States

[b]Department of Chemistry, Memorial University, St. John's, Newfoundland and Labrador, Canada A1B 3X7

ABSTRACT: Solid-state NMR (ssNMR) and ab initio quantum mechanical calculations are used in order to understand and to better characterize the molecular conformation and properties of [2.2]paracyclophane and 1,8-dioxa[8](2,7)pyrenophane. Both molecules are cyclophanes, consisting of an aromatic ring assembly and a cyclic aliphatic chain connected to both ends of the aromatic portion. The aliphatic chain causes curvature in the six-membered aromatic ring structures. This led us to examine how the ring strain due to curvature affects the chemical shifts. Using X-ray structures of both [2.2]paracyclophane and 1,8-dioxa[8](2,7)pyrenophane as our starting model, we calculate the chemical shielding tensors and compare these data with those collected from the ^{13}C ssNMR FIREMAT experiment. We define curvature of [2.2]paracyclophane and 1,8-dioxa[8](2,7)pyrenophane using the π-orbital axis vector (POAV) pyramidalization angle (θ_p).

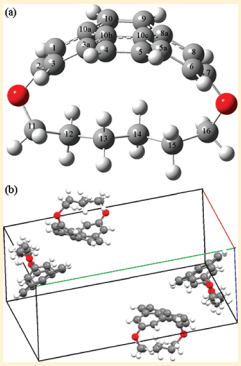

INTRODUCTION

Cyclophanes are unique molecules consisting of one or more aromatic ring systems that are bridged by one or more aliphatic chains. In many cases, the aromatic ring constituents prefer to be in a planar geometry but are forced to adopt a nonplanar (curved) geometry in whole or in part by the constraints of the aliphatic bridging unit(s).[1] There have been studies on the molecular strain on polycyclic aromatic hydrocarbons (PAHs) due to curvature.[2,3] One of the most sensitive means for determining strain in PAHs is solid-state NMR chemical shift tensors.

Solid-state NMR spectroscopy has the capability of providing full structural information with atom-level resolution.[4] It has been used to identify various distorted structures.[5,6] Chemical shift tensors have been used to determine many polycyclic aromatic hydrocarbon structures and provide useful information regarding their three-dimensional structure.[7−9] The chemical shift tensors provide electronic information for each atom in a given molecule.[10] This information includes distortions in the electron configuration due to bonding and neighboring atoms, including variations in atomic orbitals due to strain. Molecular strain caused by curvature is typically most pronounced in the δ_{33} principal component in the chemical shift tensor.[2,3] It is suggested that these distortions are due to the δ_{33} component being influenced primarily by the σ-electrons in an otherwise planar molecule, but as curvature is introduced, the π-electrons also influence δ_{33}.

Local three-dimensional curvature has been described by use of π-orbital axis vector (POAV) pyramidalization angles (θ_p) since 1986.[11,12] The POAV is defined as the vector that creates three equivalent angles ($\theta_{\sigma\pi}$) from bisecting the pyramid formed at the apex of an sp^2 carbon atom and its three protruding σ-bonds. Data for θ_p have been reported for many curved molecules, including C_{60}, and similar PAHs.[13−15]

Cyclophane structures are of interest to researchers for numerous reasons including their aromatic character, molecular strain, and curved aromatic systems.[16−18] The use of pyrene-based cyclophanes as possible synthetic precursors to fullerene substructures has also been postulated.[19] Thus, many cyclophane structures have been synthesized and studied.[16−20] One way to measure strain in cyclophane structures is to compare the curved cyclophane structure to that of its planar aromatic constituent. This can be done by comparing energetic, geometric, and magnetic properties. In this study, comparisons of chemical shift tensors will be made between 1,8-dioxa[8]-(2,7)pyrenophane (pyrenophane) and pyrene. These comparisons will provide useful information regarding ring strain introduced by forcing curvature upon molecules that energetically prefer to be planar. This information should provide further understanding of fullerenes and nanotubes along with related nonplanar aromatic compounds. Also included are the experimentally and theoretically determined chemical shift tensors of [2.2]paracyclophane.

[2.2]Paracyclophane is made up of two parallel para-substituted benzene rings that are connected via two $(CH_2)_2$ bridges as shown in Figure 1. These CH_2 bridges introduce curvature to both benzene rings. In the crystal structure of [2.2]paracyclophane, originally reported by Lonsdale et al.,[21] it was found that [2.2]paracyclophane belongs to the *P*42/*mnm* space group, has D_{2h} symmetry, and is in an eclipsed geometric

Received: October 26, 2011
Revised: April 2, 2012
Published: April 5, 2012

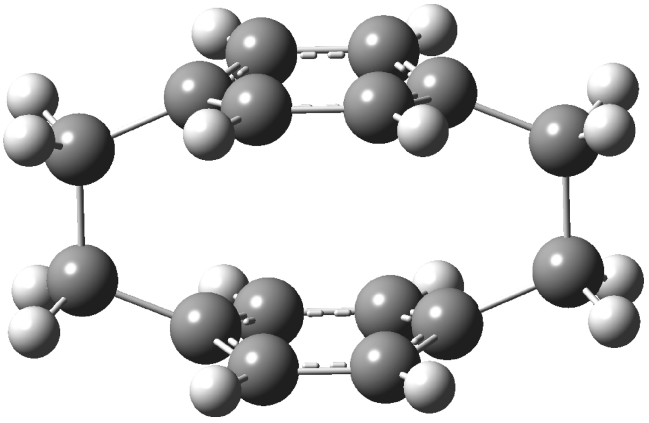

Figure 1. [2.2]paracyclophane structure reported by Lonsdale et al.[21].

conformation.[21] Theoretical studies have been performed, optimizing the energy of [2.2]paracyclophane in order to compare theoretical structures to experimental crystal structural data.[22]

The numbering scheme for pyrenophane is shown in Figure 2a. Pyrenophane is a cyclophane made up of one 2,7-disubstituted pyrene unit that is bridged by an $O(CH_2)_6O$ diether, as shown in Figure 2a. There is substantial curvature in the pyrene moiety of pyrenophane due to the strain introduced by the aliphatic bridge.[20] The single-crystal X-ray structural data for pyrenophane have been previously reported and deposited with the Cambridge Crystallographic Data Center.[20] Figure 2b shows the structure of the unit cell.

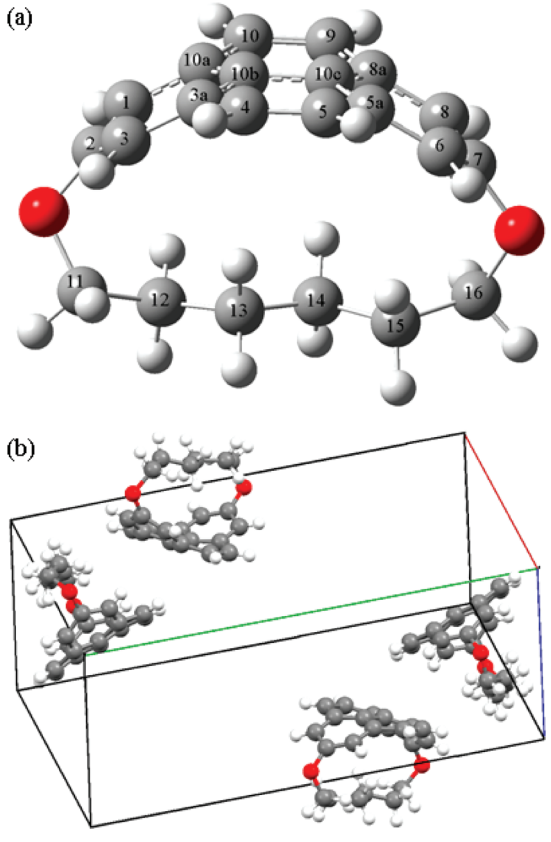

Figure 2. 1,8-Dioxa[8](2,7)pyrenophane: (a) single molecule with numbering scheme and (b) unit cell containing four molecules.

EXPERIMENTAL SECTION

Synthesis. The synthesis of pyrenophane was carried out by the Graham Bodwell laboratory group at Memorial University, Canada. Details of the synthesis and the crystal structure of pyrenophane are reported in the literature.[20] [2.2]-Paracyclophane sample was purchased from Aldrich.

Solid-State NMR. The ^{13}C FIREMAT (5π replicated magic-angle tuning) data were collected on a CMX-400 NMR spectrometer operating at 400.119 MHz for ^{1}H and 100.622 MHz for ^{13}C, using a 7.5 mm PENCIL rotor probe. The methyl peak of hexamethylbenzene (HMB) at 17.35 ppm, as referenced to tetramethylsilane (TMS), was used for referencing and setting the Hartmann–Hahn match.[23] All data were collected at room temperature at the University of Utah.

The FIREMAT data for both samples were collected by utilizing a spinning speed of 1634 Hz and the FIREMAT pulse sequence.[24] Both samples also had a contact time of 3.0 ms and spectral widths of 24.5098 and 55.5556 kHz in the evolution and acquisition dimensions, respectively. Analysis of the FIREMAT spectra used 2048 transients collected during 15 evolution increments. For the [2.2]paracyclophane sample, the other FIREMAT parameters include a recycle time of 400 s, a 4.10 μs ^{1}H 90° pulse, and a 9.10 μs ^{13}C 180° pulse. For the pyrenophane sample, the other FIREMAT parameters include a recycle time of 60 s, a 4.35 μs ^{1}H 90° pulse, and a 9.50 μs ^{13}C 180° pulse.

Data Analysis. The 1D ^{13}C isotropic guide spectrum was derived in the prescribed manner from the FIREMAT data via Fourier transformation of the evolution points corresponding to the first acquisition point according to Gan's P2DSS suppression method.[25] Side-band patterns for each of the isotropic values in the guide spectrum were calculated and fit via the TIGER processing method.[26]

Calculations. The calculations presented in this article used the X-ray data of [2.2]paracyclophane[21] and pyrenophane[20] as starting structural models. The crystal structures were refined by optimization of the hydrogen atom positions by use of the Gaussian03 suite of programs[27] utilizing density functional theory (DFT) with the B3LYP exchange and correlation functionals[28,29] as described by Cheeseman and co-workers,[30,31] along with the 6-311G** basis set,[32,33] following previously established precedents.[34,35] All of the chemical shielding calculations presented in this article were performed with the Gaussian03 suite of programs[27] utilizing the same level of theory and basis set as those used in the crystal structure refinement process. The chemical shielding tensor principal values were calculated by the gauge-independent atomic orbitals (GIAO) method and referenced to a bare nucleus.[36,37]

There have been recent improvements in the procedures for calculating chemical shielding tensors.[38] However, the B3LYP/6-311G** calculations provided sufficiently accurate tensors to assign carbon atom location with high statistical confidence at all positions examined. A detailed comparison of other tensor computation methods is given elsewhere.[39] We note that the B3LYP method suffers from systematic errors in the calculation of tensor values.[40] This is presumed to be due to its inability to fully account for electron correlation. Other tensor computation methods have also been found to suffer from systematic errors, and methods for compensating for these inaccuracies are described elsewhere.[39,41]

dx.doi.org/10.1021/jp210297c | J. Phys. Chem. A 2012, 116, 5193–5198

A simplified force field method[42] was also used to test the general applicability of obtaining approximate structures of highly strained molecular systems. This analysis was performed by use of Gaussian03 and unrestricted force field (UFF) molecular mechanics level of theory,[42] to optimize the hydrogen atom positions of the crystal structure. NMR calculations were also performed on the basis of the molecular mechanics optimization refined crystal structure.[36,37]

RESULTS AND DISCUSSION

The FIREMAT spectra for [2.2]paracyclophane and pyrenophane are given in Figures 3 and 4, respectively. The

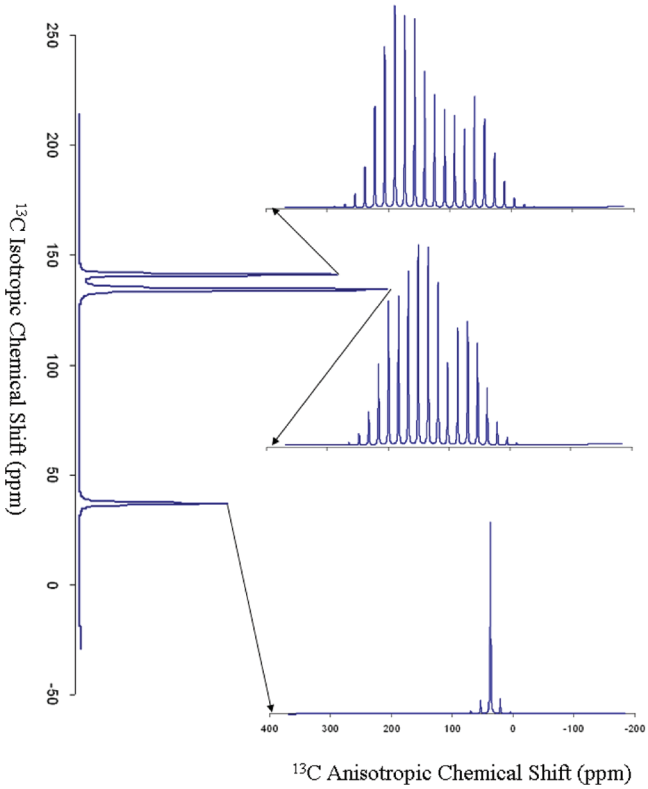

Figure 3. FIREMAT spectrum of [2.2]paracyclophane. The isotropic guide spectrum and the spinning side bands for each carbon atom are represented along the *y*- and *x*-axes, respectively.

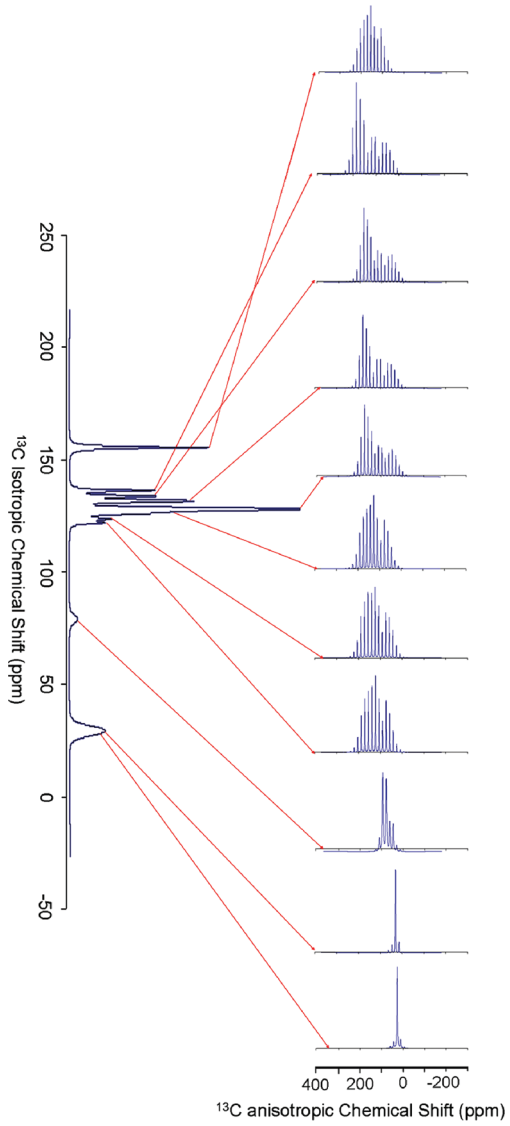

Figure 4. FIREMAT spectrum of 1,8-dioxa[8](2,7)pyrenophane. The isotropic guide spectrum and the spinning side bands for each carbon atom are represented along the *y*- and *x*-axes, respectively.

experimental and theoretical chemical shift tensor principal values of [2.2]paracyclophane and pyrenophane are reported in Tables 1 and 2, respectively. The experimental carbon tensor assignments were made, aided by the theoretical chemical shift results. All of the error values reported in this article are calculated by the root-mean-square (rms) distance metric analysis approach introduced and discussed in detail by Alderman et al.[43] and Grant and Halling.[44]

The correlation between experimental and theoretical data of [2.2]paracyclophane and pyrenophane is shown in Figure 5. The error between experiment and theory for [2.2]-paracyclophane is 2.0 ppm, whereas that for pyrenophane is 4.2 ppm. These results show excellent agreement between the theoretical chemical shielding and experimental chemical shift data.[43,44] The model used for the hydrogen geometry optimization and the theoretical NMR chemical shifts belong to the $P2_1/C$ space group symmetry; therefore, each carbon atom in pyrenophane is unique.[20] One advantage of using solid-state NMR to analyze pyrenophane (also true for [2.2]-paracyclophane) is that it provides more information regarding its three-dimensional structure than solution NMR. The FIREMAT experiment provides a means for obtaining three chemical shift principal values for each carbon atom position.[24] For pyrenophane, the chemical shift tensors are compared to their planar PAH constituent counterparts in pyrene.[45] A comparative depiction of the changes in each of the chemical shift principal components of the carbon atoms for pyrenophane is given in Figure 6. The chemical shift principal components for pyrene are also included in Figure 6 for basis of comparison.[45]

The crystal structure of pyrene shows that it is symmetrical, while the crystal structure of pyrenophane shows a slight deviation from symmetry in the pyrene constituent. This is due to the lattice of the crystal structure, which belongs to the $P2_1/C$ space group, indicating that the 22 carbon atoms are distinct and not related through symmetry. While each carbon atom is distinct, they are similar to one another, which is manifest in the closeness of the peaks in the FIREMAT guide spectrum.

dx.doi.org/10.1021/jp210297c | J. Phys. Chem. A 2012, 116, 5193−5198

Table 1. [2.2]Paracyclophane Chemical Shift Tensor Data[a]

	experimental chemical shift (ppm)				theoretical chemical shift (ppm)			
carbon	δ_{11}	δ_{22}	δ_{33}	δ_{iso}	δ_{11}	δ_{22}	δ_{33}	δ_{iso}
C	240.3	173.5	9.4	141.1	239.6	172.7	10.2	140.8
CH	231.6	148.2	23.4	134.4	234.8	143.4	22.5	133.6
CH_2	52.0	35.6	23.3	37.0	55.2	39.1	22.3	38.9

[a]The rms distance error between the experimental chemical shift and theoretical chemical shielding is ±2.0 ppm.

Table 2. 1,8-Dioxa[8](2,7)pyrenophane Chemical Shift Tensor Data[a]

	experimental chemical shift (ppm)				theoretical chemical shift (ppm)			
carbon	δ_{11}	δ_{22}	δ_{33}	δ_{iso}	δ_{11}	δ_{22}	δ_{33}	δ_{iso}
C1	211.2	138.7	21.5	123.8	214.5	133.8	31.5	126.6
C2	233.4	163.0	69.6	155.3	231.3	164.0	68.1	154.4
C3	206.8	131.9	27.2	122.0	205.8	130.6	26.4	120.9
C3a	213.8	185.5	9.7	136.3	214.9	184.7	11.8	137.1
C4	211.7	138.0	31.1	126.9	216.4	126.4	31.1	124.6
C5	211.7	138.0	31.1	126.9	214.9	133.8	31.9	126.9
C5a	206.5	181.0	7.1	131.5	206.8	177.9	10.5	131.7
C6	211.2	138.7	21.5	123.8	215.9	135.7	32.6	128.1
C7	233.4	163.0	69.6	155.3	235.2	163.3	70.3	156.3
C8	206.8	131.9	27.2	122.0	201.6	125.1	25.4	117.3
C8a	213.9	178.2	9.1	133.7	209.7	180.9	4.6	131.7
C9	211.7	138.0	31.1	126.9	220.0	125.7	30.5	125.4
C10	211.7	138.0	31.1	126.9	219.3	127.7	30.8	125.9
C10a	206.5	181.0	7.1	131.5	207.2	182.2	6.7	132.0
C10b	211.9	171.6	0.8	128.1	202.8	190.8	−6.0	129.2
C10c	211.9	171.6	0.8	128.1	202.6	188.4	−5.6	128.5
C11	101.5	101.5	31.7	78.2	105.6	94.8	31.5	77.3
C12	45.0	21.3	15.3	27.2	43.1	30.5	10.8	28.1
C13	50.7	20.2	20.2	30.4	49.6	27.3	18.0	31.6
C14	50.7	20.2	20.2	30.4	46.9	25.8	12.4	28.4
C15	45.0	21.3	15.3	27.2	45.2	30.4	15.8	30.4
C16	101.5	101.5	31.7	78.2	109.4	93.2	32.1	78.2

[a]The rms distance error between the experimental chemical shift and the theoretical chemical shielding is ±4.2 ppm.

The unrestricted force field hydrogen optimization calculations provided accurate results with no significant difference in crystal structure between DFT and UFF methods. The rms error in the two NMR chemical shielding calculations approaches, using DFT and UFF hydrogen optimization, is only 2.0 ± 0.2 ppm. Comparison of the results from hydrogen optimization by both methods produces an rms deviation of 0.007 Å for the bond lengths, 1.2° for the geminal angles, and 1.9° for the dihedral angles. Therefore, utilizing a method, such as UFF, for the hydrogen optimization calculations and coupling those results with a more exhaustive DFT NMR calculation produces results that do not differ significantly from calculations utilizing DFT throughout the entire calculation process.

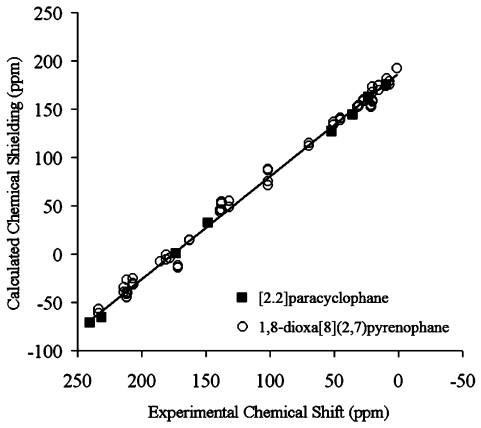

Figure 5. Correlation between theoretical chemical shielding and experimentally derived chemical shift for [2.2]paracyclophane and 1,8-dioxa[8](2,7)pyrenophane. The equation of the linear least-squares fit is $y = -1.06x + 186.4$. The R^2 value for the data is 0.996, indicating an excellent correlation between experiment and theory.

The δ_{33} component of the chemical shift tensor has been observed to be the most sensitive to ring deformation in PAHs.[2] This is believed to be due to the δ_{33} component in a planar PAH reflecting σ-electron contribution only. As curvature is added to the molecule, the π-electrons have a greater influence on the δ_{33} chemical shift component. The π-electron contribution to the δ_{33} chemical shift causes a downfield shift compared with a planar PAH. It has been reported that the greater the shift of the δ_{33} component signals more curvature or strain.[3]

The C2 and C7 carbon atoms in pyrenophane are experiencing a δ_{33} shift of 69.6 ppm compared to a value of 4.0 ppm in pyrene for the corresponding carbon atom. Theory also calculates high δ_{33} shift values of 68.1 and 70.3 ppm at the C2 and C7 positions of pyrenophane. Approximately 60 ppm of that shift is due to the attached oxygen atoms. The other

dx.doi.org/10.1021/jp210297c | J. Phys. Chem. A 2012, 116, 5193−5198

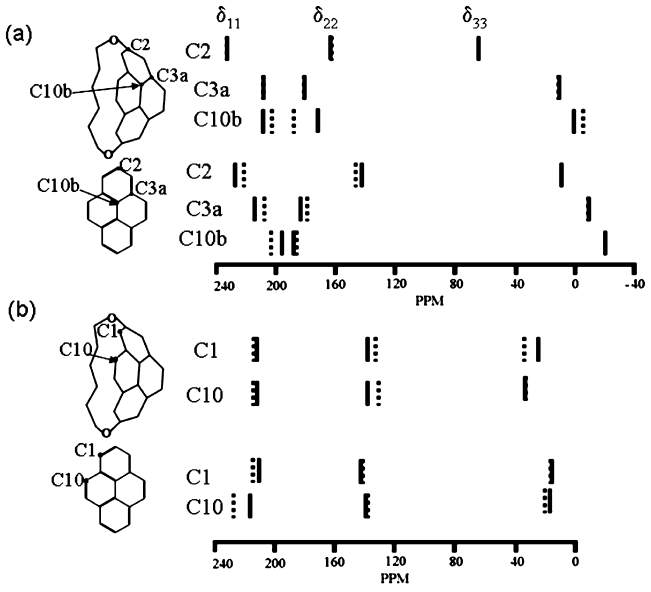

Figure 6. Experimental (|) and theoretical (⋮) ^{13}C chemical shift principal components for (a) nonprotonated and (b) protonated carbon atoms in 1,8-dioxa[8](2,7)pyrenophane, as well as corresponding chemical shift components for pyrene given for a basis of comparison. The values for benzene and pyrene were reported by Carter et al.[45].

nonprotonated carbon atoms in pyrenophane show a significant downfield δ_{33} shift in experimental chemical shift when compared with the corresponding carbons in planar pyrene, ranging between +14.1 and +18.8 ppm. This effect can be ascribed to ring strain and curvature in the pyrenophane structure. The protonated carbon atoms of pyrenophane also show significant downfield δ_{33} experimental chemical shift when compared with their corresponding carbons in planar pyrene, ranging between +0.5 and +10.1 ppm. The changes in each of the principal values are shown in Figure 6.

The theory also accurately calculates the significant downfield change in δ_{33} chemical shift tensor component for each carbon atom when pyrenophane and planar pyrene are compared. The changes in δ_{33} in theoretical chemical shifts of pyrenophane, when compared with the corresponding carbons in planar pyrene, range between +15.0 and +26.8 ppm for the nonprotonated carbon atoms. The protonated carbon atoms of pyrenophane also show similar downfield δ_{33} theoretical chemical shifts when compared with their corresponding carbons in planar pyrene, ranging between +6.4 and +23.8 ppm. These downfield shifts in δ_{33} are attributable to curvature and ring strain and show how accurately theory predicts the extent of perturbation caused by these phenomena. The changes in each of the principal values are shown in Figure 6.

The curvature at the individual carbon atom locations in [2.2]paracyclophane and pyrenophane is reported in Table 3. [2.2]Paracyclophane shows a small amount of curvature, θ_p= 2.50° and 3.00° for CH and C, respectively, while pyrenophane shows more pronounced curvature. The greatest curvature (θ_p = 5.16°) for pyrenophane is that of C10b and C10c. This compares to 11.64° for C_{60} and 8.70° for sumanene.[13] The protonated carbons in pyrenophane have θ_p values of 2.79° for C2 and C7 and 4.40° for C3a, 5a, 8a, and 10a, indicating less curvature than for C10b and C10c. The protonated carbons in pyrenophane have θ_p values of 3.50° for C1, C3, C6, and C8 and 2.19° for C4, C5, C9, and C10.

Table 3. Curvature Calculated Values for sp^2-Hybridized Carbon Atoms[a]

carbon	θ_p (deg)
1,8-Dioxa[8](2,7)pyrenophane	
1, 3, 6, 8	3.50
2, 7	2.79
4, 5, 9, 10	2.19
3a, 5a, 8a, 10a	4.40
10b, 10c	5.16
[2.2]Paracyclophane	
C	3.00
CH	2.50
C_{60}	
	11.64
Sumanene	
	8.70

[a]The values for C_{60} and sumanene are included for a basis of comparison and are reported by Haddon and co-workers.[12,13].

CONCLUSION

The solid-state NMR data for [2.2]paracyclophane and pyrenophane provide structural information regarding three-dimensional shape and structure. This information includes chemical shift tensors, which give information about the three-dimensional chemical shift anisotropy of each carbon atom. The theoretical results aided in making experimental assignments of tensors. The downfield shift of the δ_{33} component of the chemical shift tensors in pyrenophane indicates ring strain due to curvature when compared with the corresponding carbon atoms in planar pyrene. The theoretical data also accurately predict the magnitude of the downfield shift of the δ_{33} component. The POAV pyramidalization angles, θ_p, for the carbon atoms in pyrenophane also indicate a moderate amount of curvature. The solid-state NMR results for [2.2]-paracyclophane and pyrenophane reported in this paper are supported by excellent correlation with theoretical results.

AUTHOR INFORMATION

Corresponding Author

*David M. Grant, Emeritus Distinguished Professor of Chemistry, Henry Eyring BLDG 315 South 1400 East RM 2020, Salt Lake City, UT 84112. E-mail: grant@chem.utah.edu.

Notes

The authors declare no competing financial interest.

REFERENCES

(1) (a) Smith, B. H. *Bridged Aromatic Compounds*; Academic Press: New York, 1964. (b) *Cyclophanes*; Keehn, P. M., Rosenfeld, S. M., Eds.; Academic Press: New York, 1983; Vols. *1* and *2*. (c) Vögtle, F., Ed.; *Cyclophanes I and II*; Topics in Current Chemistry, Vols. *113* and *115*; Springer-Verlag: Berlin, Heidelberg, and New York, 1983 (d) Diederich, F. *Cyclophanes*; Royal Society of Chemistry: London, 1991. (e) Vögtle, F. *Cyclophane Chemistry*; Wiley: New York, 1993. (f) Weber, E., Ed.; *Cyclophanes*; Topics in Current Chemistry, Vol. *172*; Springer-Verlag: Berlin, Heidelberg, and New York 1994. (g) Kane, V. V.; de Wolf, W. H.; Bickelhaupt, F. *Tetrahedron* **1994**, *50*, 4575−4622. (h) Bodwell, G. J. *Angew. Chem., Int. Ed.* **1996**, *35*, 2085−2088. (i) de Meijere, A.; König, B. *Synlett* **1997**, 1221−1232. (j) Bodwell, G. J. in *Organic Synthesis Highlights*; Schmalz, H. G., Ed.; Wiley−VCH: New York, 2000; Vol. *IV*, pp 289−300. (k) Hopf, H. *Classics in Hydrocarbon Chemistry*; Wiley−VCH: Weinheim, Germany, 2000. (l) *Modern Cyclophane Chemistry*; Gleiter, R., Hopf, H., Eds.; Wiley−VCH: Weinheim, Germany, 2004.

(2) Iuliucci, R. J.; Phung, C. G.; Facelli, J. C.; Grant, D. M. *J. Am. Chem. Soc.* **1998**, *120*, 9305.
(3) Halling, M. D.; Orendt, A. M.; Strohmeier, M.; Solum, M. S.; Tsefrikas, V. M.; Hirao, T.; Scott, L. T.; Pugmire, R. J.; Grant, D. M. *Phys. Chem. Chem. Phys.* **2010**, *12*, 7934.
(4) Orendt, A. M. In *Encyclopedia of NMR*; Grant, D. M., Harris, R. K., Eds.; John Wiley & Sons: London, 2002; pp 551.
(5) Tycko, R.; Dabbagh, G.; Fleming, R. M.; Haddon, R. C.; Makhija, A. V.; Zahurak, S. M. *Phys. Rev. Lett.* **1991**, *67*, 1886.
(6) Yannoni, C. S.; Johnson, R. D.; Meijer, G.; Bethune, D. S.; Salem, J. R. *J. Phys. Chem.* **1991**, *95*, 9.
(7) (a) Carter, C. M.; Alderman, D. W.; Facelli, J. C.; Grant, D. M. *J. Am. Chem. Soc.* **1987**, *109*, 2639. (b) Sherwood, M. H.; Facelli, J. C.; Alderman, D. W.; Grant, D. M. *J. Am. Chem. Soc.* **1991**, *113*, 750. (c) Iuliucci, R. J.; Facelli, J. C.; Alderman, D. W.; Grant, D. M. *J. Am. Chem. Soc.* **1995**, *117*, 2336. (d) Iuliucci, R. J.; Phung, C. G.; Facelli, J. C.; Grant, D. M. *J. Am. Chem. Soc.* **1996**, *118*, 4880. (e) Iuliucci, R. J.; Phung, C. G.; Facelli, J. C.; Grant, D. M. *J. Am. Chem. Soc.* **1998**, *120*, 9305.
(8) Orendt, A. M.; Facelli, J. C.; Bai, S.; Rai, A.; Gossett, M.; Scott, L. T.; Boerio-Goates, J.; Pugmire, R. J.; Grant, D. M. *J. Phys. Chem. A* **2000**, *104*, 149.
(9) (a) Barich, D. H.; Orendt, A. M.; Pugmire, R. J.; Grant, D. M. *J. Phys. Chem. A* **2000**, *104*, 8290. (b) Barich, D. H.; Hu, J. Z.; Pugmire, R. J.; Grant, D. M. *J. Phys. Chem. A* **2002**, *106*, 6477.
(10) Harper, J. K.; McGeorge, G.; Grant, D. M. *J. Am. Chem. Soc.* **1999**, *121* (27), 6488.
(11) Haddon, R. C. *J. Am. Chem. Soc.* **1987**, *109*, 1676.
(12) Haddon, R. C.; Scott, L. T. *Pure Appl. Chem.* **1986**, *58*, 137.
(13) (a) Haddon, R. C. *Science* **1993**, *261*, 1545. (b) Haddon, R. C. *J. Am. Chem. Soc.* **1997**, *119*, 1797.
(14) Haddon, R. C. *J. Am. Chem. Soc.* **1990**, *112*, 3385.
(15) Dinadayalane, T. C.; Sastry, G. N. *Tetrahedron* **2003**, *59*, 8347.
(16) Dobrowolski, M. A.; Cyranski, M. K.; Merner, B. L.; Bodwell, G. J.; Wu, J. I.; Schleyer, P. v R. *J. Org. Chem.* **2008**, *73*, 8001.
(17) Bodwell, G. J.; Miller, D. O.; Vermeij, R. J. *Org. Lett.* **2001**, *3*, 2093.
(18) Aprahamian, I.; Bodwell, G. J.; Fleming, J. J.; Manning, G. P.; Mannion, M. R.; Merner, B. L.; Sheradsky, T.; Vermeij, R. J.; Rabinovitz, M. *J. Am. Chem. Soc.* **2004**, *126*, 6765.
(19) Bodwell, G. J.; Fleming, J. J.; Mannion, M. R.; Miller, D. O. *J. Org. Chem.* **2000**, *65*, 5360.
(20) Bodwell, G. J.; Bridson, J. N.; Houghton, T. J.; Kennedy, J. W. J.; Mannion, M. R. *Angew. Chem., Int. Ed. Engl.* **1996**, *35*, 1320.
(21) Lonsdale, K.; Milledge, H. J.; Krishna Rao, K. V. *Proc. R. Soc. London, Ser. A.* **1960**, *255*, 82.
(22) Caramori, G. F.; Galembeck, S. E.; Laali, K. K. *J. Org. Chem.* **2005**, *70*, 3242.
(23) Hartmann, S. R.; Hahn, E. L. *Phys. Rev.* **1962**, *128*, 2042.
(24) Alderman, D. W.; McGeorge, G.; Hu, J. Z.; Pugmire, R. J.; Grant, D. M. *Mol. Phys.* **1998**, *95*, 1113.
(25) (a) Gan, Z. *J. Am. Chem. Soc.* **1992**, *114*, 8307. (b) Gan, Z. *J. Magn. Reson.* **1994**, *109*, 253.
(26) (a) McGeorge, G.; Hu, J. Z.; Mayne, C. L.; Alderman, D. W.; Pugmire, R. J.; Grant, D. M. *J. Magn. Reson.* **1997**, *129*, 134. (b) Manassen, Y.; Navon, G.; Moonen, C. T. W. *J. Magn. Reson.* **1987**, *72*, 551. (c) Manassen, Y.; Navon, G. *J. Magn. Reson.* **1988**, *79*, 291.
(27) Frisch, M. J.; Trucks, G. W.; Schlegel, H. B., et al. *Gaussian03*; Gaussian, Inc., Pittsburgh, PA, 1998 and 2003.
(28) Becke, A. D. *Phys. Rev. A* **1988**, *38*, 3098.
(29) Becke, A. D. *J. Chem. Phys.* **1993**, *98*, 5648.
(30) Cheeseman, J. R.; Trucks, G. W.; Keith, T. A.; Frisch, M. J. *J. Chem. Phys.* **1996**, *104*, 5497.
(31) Wiberg, K. B.; Hammer, J. D.; Zilm, K. W.; Cheeseman, J. R. *J. Org. Chem.* **1999**, *64*, 6394.
(32) McLean, A. D.; Chandler, G. S. *J. Chem. Phys.* **1980**, *72*, 5639.
(33) Krishnan, R.; Binkley, J. S.; Seeger, R.; Pople, J. A. *J. Chem. Phys.* **1980**, *72*, 650.
(34) Grant, D. M.; Liu, F.; Iuliucci, R. J.; Phung, C. G.; Facelli, J. C.; Alderman, D. W. *Acta Crystallogr.* **1995**, *B51*, 540.
(35) Facelli, J. C. *Concepts Magn. Reson.* **2004**, *20A*, 42.
(36) Ditchfield, R. *J. Chem. Phys.* **1972**, *56*, 5688.
(37) Pulay, P.; Hinton, J. F. In *Encyclopedia of NMR*; Grant, D. M., Harris, R. K., Eds.; John Wiley & Sons: London, 1996; pp 4334.
(38) (a) Sebastiani, D.; Parrinello, M. *J. Phys. Chem. A* **2001**, *105*, 1951. (b) Pickard, C. J.; Mauri, F. *Phys. Rev. B* **2001**, *63*, No. 245101. (c) Perdew, J. P.; Burke, K.; Ernzerhof, M. *Phys. Rev. Lett.* **1997**, *78*, 1396. (d) Keal, T. W.; Tozer, D. J. *J. Chem. Phys.* **2003**, *119*, 3015. (e) Teale, A. M.; Tozer, D. *J. Chem. Phys. Lett.* **2004**, *383*, 109. (f) Yates, J. R.; Pickard, C. J.; Mauri, F. *Phys. Rev. B* **2007**, *76*, No. 024401.
(39) (a) Sefzik, T. H.; Fidler, J. M.; Iuliucci, R. J.; Facelli, J. C. *Magn. Reson. Chem.* **2006**, *44*, 390. (b) Sefzik, T. H.; Turco, D.; Iuliucci, R. J.; Facelli, J. C. *J. Chem. Phys. A* **2005**, *109*, 1180. (c) Johnston, J. C.; Liliucci, R. J.; Facelli, J. C.; Fitzgerald, G.; Mueller, K. T. *J. Chem. Phys.* **2009**, *131*, No. 144503.
(40) (a) Harper, J. K.; McGeorge, G.; Grant, D. M. *J. Am. Chem. Soc.* **1999**, *121*, 6488. (b) Harper, J. K.; McGeorge, G.; Grant, D. M. *Magn. Reson. Chem.* **1998**, *36*, S135. (c) Harper, J. K. In *Encyclopedia of Magnetic Resonance*; Grant, D. M., Harris, R. K., Eds.; Wiley: Chichester, U.K., 2002; Vol. *9*, pp 589.
(41) Dumez, J. N.; Pickard, C. J. *J. Chem. Phys.* **2009**, *130*, No. 104701.
(42) Rappé, A. K.; Casewit, C. J.; Colwell, K. S.; Goddard, W. A., III; Skiff, W. M. *J. Am. Chem. Soc.* **1992**, *114*, 10024.
(43) Alderman, D. W.; Sherwood, M. H.; Grant, D. M. *J. Magn. Reson. A.* **1993**, *101*, 188.
(44) Grant, D. M.; Halling, M. D. *Concepts Magn. Reson. A* **2009**, *34*, 217.
(45) Carter, C. M.; Alderman, D. W.; Facelli, J. C.; Grant, D. M. *J. Am. Chem. Soc.* **1987**, *109*, 2639.